Latent heat and nonlinear vortex liquid in the vicinity of the first-order phase transition in layered high-T_c superconductors

M. I. Dolz,[1,2,*] Y. Fasano,[3] H. Pastoriza,[3] V. Mosser,[4] M. Li,[5] and M. Konczykowski[2]

[1]*Departamento de Física, Universidad Nacional de San Luis, and Instituto de Física Aplicada, CONICET, 5700 San Luis, Argentina*

[2]*Laboratoire des Solides Irradiés, Ecole Polytechnique, CNRS URA-1380, 91128 Palaiseau, France*

[3]*Low Temperature Division, Centro Atómico Bariloche, CNEA, 8400 Bariloche, Argentina*

[4]*Itron SAS, F-92448 Issy-les-Moulineaux, France*

[5]*Kamerlingh Onnes Laboratorium, Rijksuniversiteit Leiden, 2300 RA Leiden, The Netherlands*

(Received 2 June 2014; revised manuscript received 23 September 2014; published 13 October 2014)

In this work we revisit the vortex matter phase diagram in layered superconductors solving still open questions by means of ac and dc local magnetic measurements in the paradigmatic $Bi_2Sr_2CaCu_2O_8$ compound. We show that measuring with ac magnetic techniques is mandatory in order to probe the bulk response of vortex matter, particularly at high temperatures where surface barriers for vortex entrance dominate. From the T_{FOT} evolution of the enthalpy and latent heat at the transition we find that, contrary to previous reports, the nature of the dominant interlayer coupling is electromagnetic in the whole temperature range. By studying the dynamic properties of the phase located at $T \gtrsim T_{FOT}$, we reveal spanning in a considerable fraction of the phase diagram of a nonlinear vortex phase suggesting that bulk pinning might play a role even in the liquid vortex phase.

DOI: 10.1103/PhysRevB.90.144507 PACS number(s): 74.25.Uv, 74.25.Ha, 74.25.Dw

I. INTRODUCTION

One of the main features of the phase diagram of vortex matter in layered high-temperature superconductors is the occurrence of a first-order transition (FOT) [1,2] at T_{FOT} due to the relevance of thermal fluctuations at temperatures close to the critical temperature T_c. The layered nature of vortex matter in these extremely anisotropic materials plays a key role on the location of T_{FOT} and on the temperature-evolution of the main thermodynamic magnitudes at the transition. When applying a field along the sample, c-axis vortices are actually a stack of pancake vortices lying in the CuO planes, coupling between layers via electromagnetic and Josephson interactions [3]. In the case of the paradigmatic layered $Bi_2Sr_2CaCu_2O_8$ compound, the first-order transition separates a solid phase at low temperatures and a liquid [4] or decoupled gas [5] of pancake vortices with reduced shear viscosity [6] at high temperatures.

The solid phase presents irreversible magnetic behavior ascribed to bulk pinning and surface barriers, each of them dominating at different temperature and measuring-time ranges [7–9]. Direct imaging of vortices in pristine $Bi_2Sr_2CaCu_2O_8$ reveals the vortex solid has quasi-long-range positional order [10,11]. Josephson-plasma-resonance measurements indicate the T_{FOT} transition line corresponds to a single-vortex decoupling process between pancake vortices from adjacent layers within the same stack [12]. The first-order line is then a single-vortex transition that depends, at best, on the density of the surrounding vortex matter. Therefore, the relative importance of the two types of interaction between pancake vortices determines the temperature evolution of the enthalpy and latent heat, $T_{FOT}\Delta S$, of the transition.

The main thermodynamic magnitudes entailed in this transition; namely, the entropy-jump per pancake vortex, ΔS, and the enthalpy that is proportional to the observed jump in local induction, ΔB, have been investigated experimentally as well as theoretically [2,13]. A previous report claims that, for $T_{FOT} \sim T_c$, the latent heat of the transition is not satisfactorily described by considering the electromagnetic interaction as the dominant coupling mechanism between pancakes of adjacent layers [13]. The same work proposed then the existence of a crossover to a high-T_{FOT} (low-field) regime where interlayer coupling is dominated by the Josephson interaction. This statement results from interpreting data obtained from dc magnetization measurements, a technique that lacks sensibility to detect bulk currents at $T \sim T_c$.

At such high temperatures the magnetic response of $Bi_2Sr_2CaCu_2O_8$ vortex matter is dominated by geometrical or Bean–Livingston surface barriers [8,14]. Nevertheless, previous work reported on the plausibility of bulk pinning playing a role in vortex dynamics even at temperatures larger than T_{FOT}, within the vortex liquid phase [15]. Bulk pinning does play a dominant role for temperatures below $0.6T_c$, and the first-order transition is observed as the so-called second-peak effect [7,16] or order-disorder transition, H_{SP} [17–19]. This region of the transition is detected through an increase of the width of dc hysteresis loops [7], or as a minimum in ac magnetization loops, both occurring at H_{SP}, independently of frequency.

Therefore, several issues in the vortex phase diagram of layered high-temperature superconductors still remain open to discussion, such as an accurate description of the physics entailed in the first-order vortex phase transition in $Bi_2Sr_2CaCu_2O_8$. In particular, the dominant coupling between adjacent CuO planes for $T \sim T_c$, electromagnetic vs Josephson, is poorly studied in the literature. Most of the attempts to settle this issue suffered from comparing data obtained with experimental techniques lacking the proper sensibility to ascertain the relative importance of bulk effects, surface barriers, and sample inhomogeneities [2,20]. In this work, we apply ac and dc local-magnetic-measurement techniques. Our ac local magnetic measurements have a typical resolution of 5 mG, one order of magnitude better

*mdolz@unsl.edu.ar

than in the case of local dc magnetometry. By analyzing ac and dc data obtained in a collection of optimally doped samples, we rule out the proposal of a crossover between the dominance of electromagnetic to Josephson coupling taking place at low fields (high temperatures), suggesting that the dominant interaction between pancakes at T_{FOT} is always of the same nature. In addition, we report on a nonlinear liquid vortex phase spanning a considerable fraction of the high-temperature region of the phase diagram. The large extent of this phase challenges the idea of a vortex liquid being a linear phase.

II. EXPERIMENTAL

The optimally doped $Bi_2Sr_2CaCu_2O_8$ single crystals studied in this work ($T_c = 90$ K) were grown by means of the traveling-solvent floating-zone technique [21]. The local magnetization of the samples were measured with a microfabricated two-dimensional (2D) electron gas Hall-sensor array [22]. The eleven-probe array was photolithographically fabricated from GaAs/AlGaAs heterostructures and each sensor has an active area of $6 \times 6\,\mu m^2$. A schematic representation of our experimental setup is shown in Fig. 1.

Local ac magnetization measurements were performed by applying dc and ripple magnetic fields, both parallel to the c axis, H and H_{ac}, respectively. dc magnetic hysteresis loops are obtained by measuring the magnetization, $H_s = B - H$, when cycling H at fixed temperatures. In the ac measurements the ripple field has an amplitude of 0.9 Oe rms and frequencies ranging from 1 to 1000 Hz. The first and third harmonics of the ac magnetic induction are simultaneously measured by means of a digital-signal-processing lock-in technique. The in-phase component of the first-harmonic signal, B', is converted to the transmittivity $T' = [B'(T) - B'(T \ll T_c)]/[B'(T > T_c) - B'(T \ll T_c)]$ [23], a magnitude extremely sensitive to discontinuities in the local induction associated with first-order magnetic transitions. A non-negligible magnitude of the third-harmonic signal, $|T_{h3}| = |B_{h3}^{AC}|/[B'(T > T_c) - B'(T \ll T_c)]$, indicates the appearance of nonlinearities in the magnetic response. The onset of $|T_{h3}|$ upon cooling is considered as the irreversibility temperature or field, T_{IL} or H_{IL} [24].

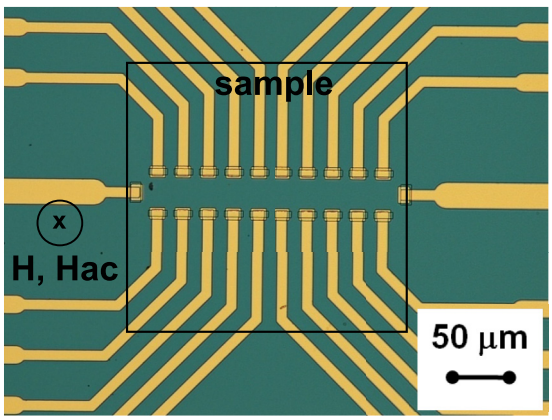

FIG. 1. (Color online) Experimental setup: real-scale $Bi_2Sr_2CaCu_2O_8$ sample ($220 \times 220 \times 30\ \mu m^3$) located on top of the 2D electron gas Hall-sensor array. dc and ripple magnetic fields, H and H_{ac}, are applied parallel to the sample c axis.

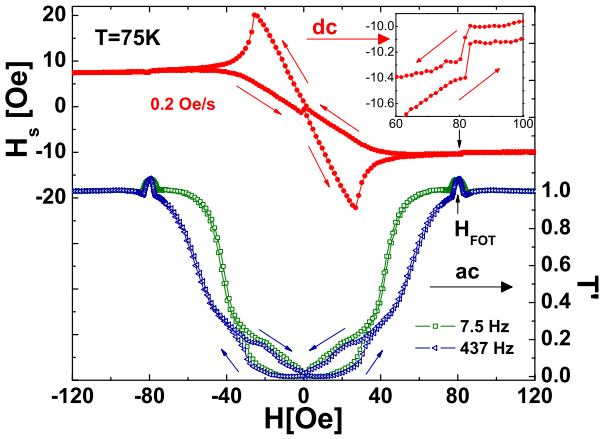

FIG. 2. (Color online) dc and ac magnetic hysteresis loops of $Bi_2Sr_2CaCu_2O_8$ sample measured at 75 K. (top) Ascending and descending branches of a dc hysteresis loop. (inset) Zoom in of the dc loop at the vicinity of the first-order transition entailing a B jump (see black arrow). Red arrows indicate the ascending and descending branches. (bottom) ac transmittivity loops with paramagnetic peaks fingerprinting the first-order transition field H_{FOT}. The loops were measured with ripple fields of 0.9 Oe rms in amplitude and frequencies of 7.5 and 437 Hz. Blue arrows indicate the ascending and descending branches.

In order to track the $H - T$ location of the first-order transition and irreversibility lines in $Bi_2Sr_2CaCu_2O_8$ vortex matter, we perform two types of measurements: Isothermal dc and ac hysteresis loops [25], and temperature evolution of T' and $|T_{h3}|$ upon field cooling at various magnetic fields (see Figs. 2 and 3). We discuss the magnetic response of our sample at three characteristic-temperature regimes of the vortex phase diagram.

III. RESULTS AND DISCUSSION

In the high-temperature regime, $T \gtrsim 0.83T_c$, the first-order transition is manifested in T' as a prominent paramagnetic peak developing at the same H_{FOT} as the jump in B detected in dc hysteresis loops [20,25]. The top panel of Fig. 2 shows a typical two-quadrant dc loop observed in this temperature regime, indicating that surface barriers dominate the vortex entrance to the sample. Closer inspection of the dc data in the vicinity of 80 Oe reveals a H_s jump with similar height for both ascending and descending branches. This feature is the fingerprint of the first-order transition H_{FOT} in the high-temperature region [2]. The bottom panel of Fig. 2 shows that, in the ac loops, this transition is detected with improved resolution: Paramagnetic peaks appear at the same fields where the H_s jumps are measured [25]. At lower fields the shielding capability is increased. Upon increasing frequency, the system enhances its shielding capability manifested as a T' decrease. The field location of the paramagnetic peak in ac loops, H_{FOT}, is frequency independent.

Figure 3(a) shows a set of ac magnetic data for applied fields up to 100 Oe. The paramagnetic peak, observed in T'

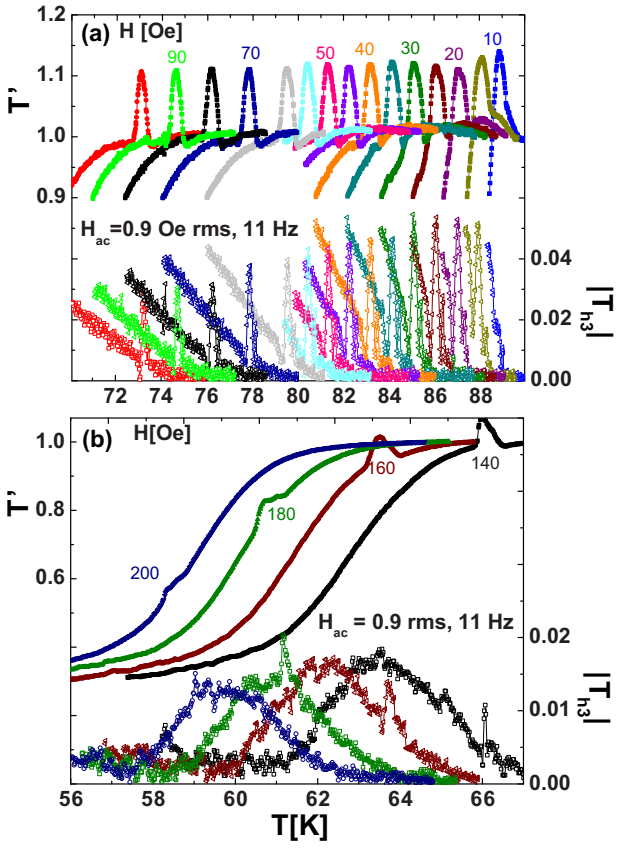

FIG. 3. (Color online) Temperature-dependence of the transmittivity and modulus of the third-harmonic response for the $Bi_2Sr_2CaCu_2O_8$ vortex matter nucleated in a field-cooling process. (a) Very-low- and (b) low-field regimes. The ac ripple field of 0.9 Oe rms and 11 Hz is collinear to the applied field H.

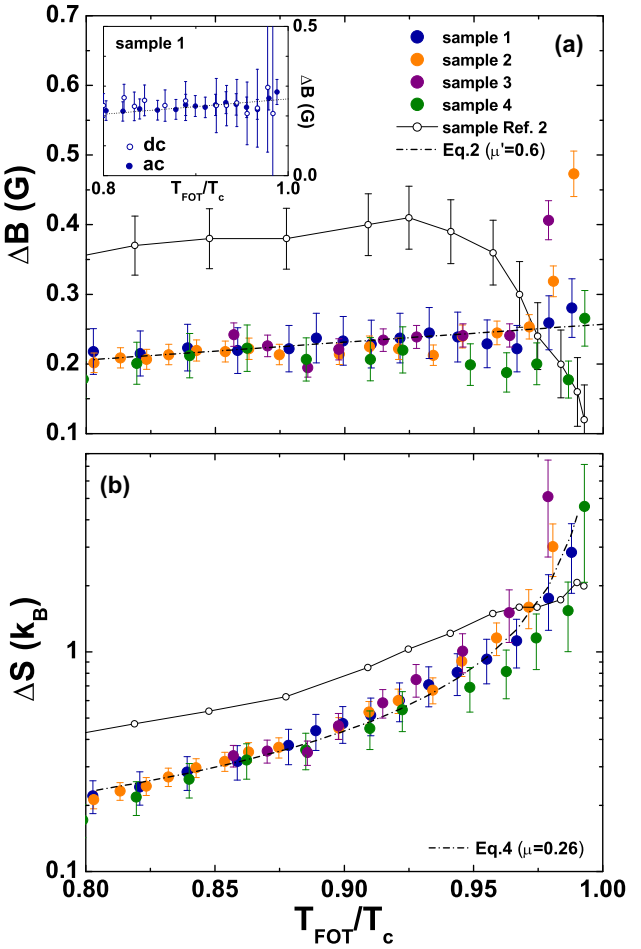

FIG. 4. (Color online) (a) Magnetic-induction jump ΔB and (b) entropy jump per pancake vortex, ΔS, at the first-order transition of $Bi_2Sr_2CaCu_2O_8$ vortex matter for several samples studied by means of ac and dc techniques in this work (full points). (inset) Comparison between the ΔB obtained by means of dc and ac measurements for the illustrative case of one of our crystals. Our data are reasonably well fit (dashed line) assuming dominant electromagnetic interactions between pancake vortices in the whole temperature range. The data from Ref. [2] obtained from dc local magnetization (open points) are plotted for comparison.

vs T measurements at $T_{\rm FOT}$, shifts towards lower temperatures upon increasing field. The peaks are sharp with an amplitude that slightly decreases upon increasing field. Figure 3(b) shows that, at fields larger than 100 Oe, shielding currents develop in the sample prior to the appearance of the paramagnetic peak. Nevertheless, the peak can be clearly detected in ac magnetic measurements up to 200 Oe.

The enthalpy of this first-order transition is proportional to the height of the step in the magnetic induction at $T_{\rm FOT}$. This magnitude can be obtained from the transmittivity value at the transition field considering that for $T \gtrsim T_{\rm FOT}$ the transmittivity $T' \sim B'/H_{\rm ac}$ and therefore [20]

$$T' = 1 + \frac{2\Delta B}{\pi H_{\rm ac}} \qquad (1)$$

for small ripple fields $H_{\rm ac}$. Figure 4(a) shows the ΔB evolution with $T_{\rm FOT}/T_{\rm c}$ obtained from applying Eq. (1) to $T'(T)$ data at different fields and for four different optimally doped pristine samples. The value of ΔB obtained in this way is equal to the one obtained in our dc magnetization loops within the error; see inset to Fig. 4(a). We found a linear increase of ΔB up to temperatures $T_{\rm FOT} \sim T_{\rm c}$ within the error bars. These findings are in contrast to the seminal work of Ref. [2] reporting that, for $T_{\rm FOT} \geqslant 0.93T_{\rm c}$, the jump in magnetic induction obtained from dc data decreases dramatically down to 25% at $T_{\rm c}$. This result was interpreted within the framework of a crossover between an electromagnetic to Josephson coupling of pancake vortices on decreasing field (increasing $T_{\rm FOT}$). This interpretation was proposed by the theoretical work of Ref. [13], that provided the functionality of $\Delta B(T)$ at the first-order transition.

A linear evolution of ΔB can be explained by considering that the interlayer coupling is dominated by electromagnetic interactions between weakly bound pancake vortices undergoing large thermal fluctuations. Taking into account the dispersive electromagnetic line tension of vortices and the Lindemann criterion for vortex melting [3,13], in this case

$$\Delta B = \mu' \frac{k_{\rm B} T_{\rm FOT}}{\phi_0 d}, \qquad (2)$$

where $k_{\rm B}$ is the Boltzmann constant, ϕ_0 is the flux quantum, $d \approx 15$ Å is the CuO-plane interlayer distance, and μ' is a numerical constant [13]. The latter constant depends on the

Lindemann number for a given material and, to the best of our knowledge, there is no report of its quantitative value in the case of $Bi_2Sr_2CaCu_2O_8$. The linear ΔB data obtained in our sample are reasonably well fit with Eq. (2) for $\mu' = 0.6$. A follow-on paper of Ref. [13] proposed that, if taking into account only electromagnetic interactions, μ is a temperature-dependent parameter [26]. Our data are not properly fit with the temperature-dependence proposed for μ in Ref. [26]. However the mentioned theoretical work does not take into account the effect of pinning present in real samples.

The entropy-jump per vortex and per CuO layer entailed in the first-order transition can be obtained from ΔB data by means of the thermodynamic Clausius–Clapeyron relation

$$\Delta S = -\frac{\phi_0 d}{4\pi}\frac{\Delta B}{B_{\mathrm{FOT}}}\frac{dH_{\mathrm{FOT}}}{dT}. \tag{3}$$

Figure 4(b) shows that the ΔS data of our sample diverges close to T_c, as also reported in the previous work of Ref. [2]. In order to explain the measured T_{FOT} evolution of ΔS in terms of the nature of the interlayer coupling that dominates in the system, Ref. [13] proposes that, for electromagnetic interactions,

$$\Delta S = \frac{\mu}{\pi}\frac{k_B}{[1-(T_{\mathrm{FOT}}/T_c)^2]}, \tag{4}$$

with μ being a material-dependent constant. Our ΔS data are reasonably well fit with the expression of Eq. (4) in the whole temperature range close to T_c. Therefore, our results are in discrepancy with the data and interpretation provided in Ref. [2] where the divergent ΔS was not satisfactorily fit with Eq. (4). However this might be associated with the fact that, in Ref. [2], ΔB decreases close to T_c. The difference between our data on several samples and those of the sample of the seminal work of Ref. [2] can have its origin in different levels of inhomogeneities in the samples (our samples are smaller and presumably more homogeneous).

Another remarkable phenomenology in the high-temperature region of the phase diagram is that the irreversibility temperature T_{IL} identified from the onset of the third-harmonic signal on cooling develops at temperatures larger than those associated with the paramagnetic peak [see the lower panel of Fig. 3(b)]. This indicates the existence of a phase region with nonlinear vortex dynamics at fields exceeding H_{FOT}. Previous works reported a qualitatively similar phenomenology by means of magneto-optic [15] and magnetization measurements [27]. Figure 5 shows that the spanning of this nonlinear vortex liquid phase increases with frequency and, at high fields (300 Oe), can be as large as 20% of T_c for frequencies of the order of 1 kHz. This phenomenon might have its origin in a residual effect of pinning [28], or Bean–Livingston barriers [29] on the high-temperature liquid phase.

The vortex phase diagram of Fig. 5 also shows the connection between the low-temperature regime of the first-order transition, H_{SP}, and the high-temperature regime H_{FOT} for $0.4 \lesssim T/T_c \lesssim 0.5$ [30]. The H_{SP} transition field can be obtained from dc magnetic hysteresis loops as shown in Fig. 6(a) for three different temperatures. In these curves the local minimum (maximum) of the ascending (descending) branch becomes more evident upon cooling. The loops occupy

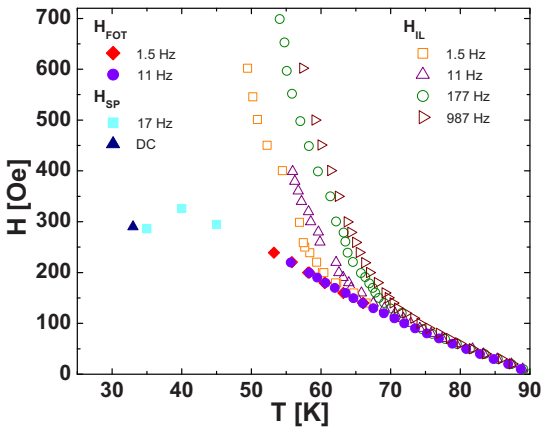

FIG. 5. (Color online) Vortex phase diagram of $Bi_2Sr_2CaCu_2O_8$ depicting the first-order transition line in the high- and low-temperature regions, H_{FOT} and H_{SP} (full points). Data were obtained from ac and dc magnetic measurements. The frequency-dependent irreversibility line, H_{IL}, is indicated with open points. All ac measurements were performed applying a ripple field with amplitude of 0.9 Oe rms.

two field quadrants and noticeably increase their width upon cooling. This figure also indicates that the H_{SP} field is hard to detect from dc magnetic loops for temperatures larger than 33 K. This is due to a technical limitation of the dc technique that lacks resolution in order to measure bulk transitions when surface barriers dominate the magnetic properties [8].

We therefore use the ac hysteresis loop technique in order to track the second-peak transition in the intermediate-temperature regime. The ac transmittivity reflects the dimensionless normalized sustainable current density $J = j(f)a/H_{\mathrm{ac}}$ from $J = (1/\pi)\arccos(2T' - 1)$ [24], with a being a typical sample dimension. The sustainable current is a measure of the critical current taking into account creep effects [24]. The dependence of J on transmittivity was derived for ac penetration in the Bean critical regime, an assumption that seems to be valid in view of the results presented in Ref. [15]. A low-temperature ac loop at 35 K is shown in Fig. 6(b), depicting local minima in both the ascending and descending branches. This minima can be ascribed to the second-peak transition H_{SP} since a minimum in T' corresponds to a maximum in the bulk J. The T' signal evolves in a different manner for the high- and intermediate-temperature regimes. For temperatures larger than $0.66T_c = 58$ K, the transmittivity presents paramagnetic peaks, developing at the flanks of the central depletion (see Fig. 3). For intermediate temperatures a sudden jump of T' is detected, as for instance in the ac loops measured at 40 and 45 K [see Fig. 6(b)]. This step-like feature, manifested at a field H_{step} implies a frequency-independent drop of the magnetic hysteresis, consistent with the change in the width of the dc loops, and indicating that this transition is governed by the local value of B rather than H [31]. The jump in T' is related to the sudden change in shielding currents with the sample becoming more transparent to the penetration of the ac ripple field at larger H. Similarly, the height of the steps in T' decreases upon increasing temperature.

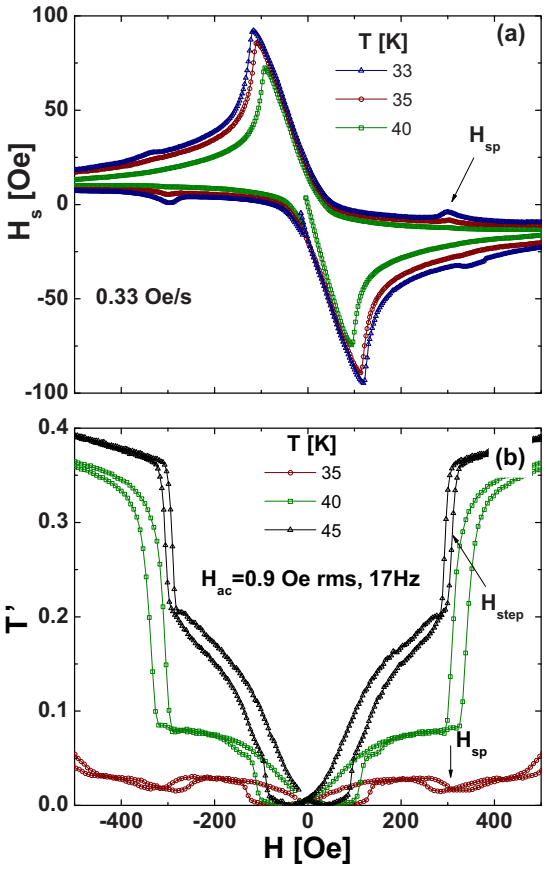

FIG. 6. (Color online) dc and ac magnetic hysteresis loops for $Bi_2Sr_2CaCu_2O_8$ vortex matter in the low-intermediate–temperature regime. (a) dc loops: the transition field H_{SP} is taken at the midpoint between the onset and the full development of the local minimum in the ascending branch. (b) Transmittivity ac loop measured with a ripple field of 0.9 Oe rms and 17 Hz parallel to H. The H_{SP} field is obtained similarly as in dc loops (see arrow). The field location of the step-like feature, H_{step}, is taken at half the step height in the ascending field branch.

The crossover temperature for the detection of the second peak [32,33], or of the step-like feature, is time and frequency dependent [8]. Figure 7 presents the evolution of the normalized sustainable-current density extracted from T' as a function of frequency in the range from 1.5 to 985 Hz. For frequencies smaller than 7.5 Hz a sudden drop of J develops at fields $H_{SP} \sim 330$ Oe. Upon increasing frequency, this feature evolves into a field-asymmetric peak producing the step-like feature observed in T' curves. The onset of this peak, or equivalently the H_{step} field in T', is frequency independent.

Thus, for $0.39T_c \approx 35\ \text{K} < T < 0.66T_c \approx 60\ \text{K}$ we detect, at a field H_{step}, a discontinuous decrease of the bulk shielding currents associated with the first-order transition. Below $T = 0.39T_c = 35$ K the opposite effect; namely, an increase of the shielding currents, is observed at almost the same field, indicating the occurrence of the H_{SP} transition. In the vicinity of this reversal of current behavior, varying the frequency of the ac ripple field tunes a decrease (low frequencies) or an increase (high frequencies) of the shielding currents. The latter case is equivalent to probing magnetic relaxation on a shorter

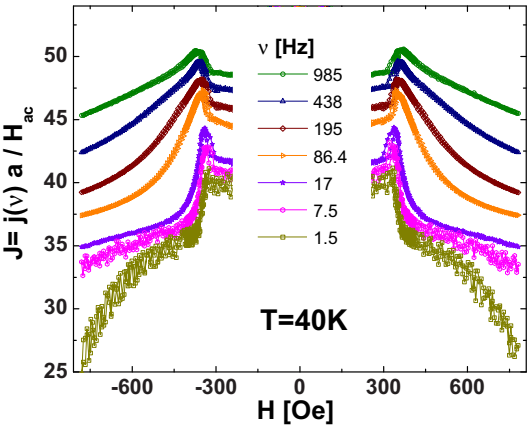

FIG. 7. (Color online) Normalized sustainable current density J as a function of applied field at 40 K. The frequency dependence of J is obtained from ac magnetization loops measured with a ripple field of 0.9 Oe rms and frequencies ranging from 1.5 to 985 Hz.

timescale, in analogy to dc magnetization experiments [8] or to choosing a higher electric field in a transport $I(V)$ measurement. Since the $I(V)$ curves just below and above the first-order transition cross—with the electric field in the high-field phase being larger than that in the low-field phase for the low-current-density limit, and vice versa for the high-current-density limit—varying the working point (by tuning the frequency) leads to either a step-like behavior of the screening current (at low electric fields) or a peak-like curve (at high electric fields) [34]. The energy barriers for flux creep have $U(J)$ and $E(J)$ curves with different functionalities for fields larger or smaller than the transition one. On varying field close to the transition these curves cross, and the phase transition produces a discontinuous change on the electrodynamics of vortex matter. Detecting the transition with a high electric field (short measurement times) leads to an enhancement of shielding currents with increasing field, whereas with a low electric field (long times) a sudden decrease is observed.

IV. CONCLUSIONS

We revisited the vortex phase diagram in pristine $Bi_2Sr_2CaCu_2O_8$ vortex matter by applying ac and dc local magnetization techniques and reveal a new phenomenology regarding the thermodynamic properties and the nature of the first-order phase transition line. We show that, in this case, ac local-magnetic techniques probe the physics at shorter timescales, having access to currents flowing in the bulk sample with improved sensitivity than dc measurements. As a consequence, we were able to track down the connection between the low H_{SP} and high H_{FOT} temperature regions of the first-order vortex phase transition in an intermediate temperature-regime, covering the whole temperature-range of the transition. By combining simultaneous measurements of the first and third harmonics of the magnetization we were also able to detect the existence of a nonlinear vortex liquid phase at $T < T_{IL}$ spanning a vortex phase region that at 300 Oe can be as large as 20 K. The width of this nonlinear liquid region increases upon increasing frequency.

From ac magnetic data we also found that, contrary to previous reports [2], the enthalpy associated with the high-temperature first-order transition, $\propto \Delta B$, increases linearly with T_{FOT} in the whole temperature range up to T_c. By means of the thermodynamic Clausius–Clapeyron relation we estimated the entropy jump per pancake vortex. We explain the temperature-evolution of the latent heat of our sample considering solely the dominance of electromagnetic interlayer coupling all along the H_{FOT} transition. This is in clear contrast to the claims of Refs. [2,13] that the dominant interlayer coupling changes nature along the H_{FOT} line upon approaching T_c.

ACKNOWLEDGMENTS

We thank C. J. van der Beek for selecting the crystals. This work was supported by the ECOS Sud-MINCyT France–Argentina collaboration program, Grant No. A09E03 and by PICT-PRH 2008-294 from the ANPCyT.

[1] H. Pastoriza, M. F. Goffman, A. Arribere, and F. de la Cruz, Phys. Rev. Lett. **72**, 2951 (1994).
[2] E. Zeldov, D. Majer, M. Konczykowski, V. B. Geshkenbein, V. M. Vinokur, and H. Shtrikman, Nature (London) **375**, 373 (1995).
[3] G. Blatter, M. V. Feigel'man, V. B. Geshkenbein, A. I. Larkin, and V. M. Vinokur, Rev. Mod. Phys. **66**, 1125 (1994).
[4] D. R. Nelson, Phys. Rev. Lett. **60**, 1973 (1988).
[5] L. I. Glazman and A. E. Koshelev, Phys. Rev. B **43**, 2835 (1991).
[6] H. Pastoriza and P. H. Kes, Phys. Rev. Lett. **75**, 3525 (1995).
[7] N. Chikumoto, M. Konczykowski, N. Motohira, K. Kishio, and K. Kitazawa, Phys. C (Amsterdam, Neth.) **185–189**, 2201 (1991).
[8] N. Chikumoto, M. Konczykowski, N. Motohira, and A. P. Malozemoff, Phys. Rev. Lett. **69**, 1260 (1992).
[9] E. Zeldov, D. Majer, M. Konczykowski, A. I. Larkin, V. M. Vinokur, V. B. Geshkenbein, N. Chikumoto, and H. Shtrikman, Europhys. Lett. **30**, 367 (1995).
[10] Y. Fasano, J. Herbsommer, and F. de la Cruz, Phys. Status Solidi B **215**, 563 (1999).
[11] Y. Fasano, M. De Seta, M. Menghini, H. Pastoriza, and F. de la Cruz, Proc. Natl. Acad. Sci. USA **102**, 3898 (2005).
[12] S. Colson, M. Konczykowski, M. B. Gaifullin, Y. Matsuda, P. Gierlowski, M. Li, P. H. Kes, and C. J. van der Beek, Phys. Rev. Lett. **90**, 137002 (2003).
[13] M. J. W. Dodgson, V. B. Geshkenbein, H. Nordborg, and G. Blatter, Phys. Rev. Lett. **80**, 837 (1998).
[14] N. Morozov, E. Zeldov, D. Majer, and B. Khaykovich, Phys. Rev. Lett. **76**, 138 (1996).
[15] M. V. Indenbom, C. J. van der Beek, V. Berseth, M. Konczykowski, N. Motohira, H. Berger, and W. Benoit, J. Low Temp. Phys. **105**, 1117 (1996).
[16] N. Avraham, B. Khaykovich, Y. Myasoedov, M. Rappaport, H. Shtrikman, D. E. Feldman, T. Tamegai, P. H. Kes, M. Li, M. Konczykowski, C. J. van der Beek, and E. Zeldov, Nature (London) **411**, 451 (2001).
[17] B. Khaykovich, M. Konczykowski, E. Zeldov, R. A. Doyle, D. Majer, P. H. Kes, and T. W. Li, Phys. Rev. B **56**, R517 (1997).
[18] V. M. Vinokur, B. Khaykovich, E. Zeldov, M. Konczykowski, R. A. Doyle, and P. H. Kes, Phys. C (Amsterdam, Neth.) **295**, 209 (1998).
[19] R. Cubitt, E. M. Forgan, G. Yang, S. L. Lee, D. M. Paul, H. A. Mook, M. Yethiraj, P. H. Kes, T. W. Li, A. A. Menovsky, Z. Tarnawski, and K. Mortensen, Nature (London) **365**, 407 (1993).
[20] N. Morozov, E. Zeldov, D. Majer, and M. Konczykowski, Phys. Rev. B **54**, R3784 (1996).
[21] T. W. Li, P. H. Kes, N. T. Hien, J. J. M. Franse, and A. A. Menovsky, J. Cryst. Growth **135**, 481 (1994).
[22] M. Konczykowski, C. J. van der Beek, M. A. Tanatar, V. Mosser, Yoo Jang Song, Yong Seung Kwon, and R. Prozorov, Phys. Rev. B **84**, 180514(R) (2011).
[23] J. Gilchrist and M. Konczykowski, Phys. C (Amsterdam, Neth.) **212**, 43 (1993).
[24] C. J. van der Beek, M. Konczykowski, V. M. Vinokur, G. W. Crabtree, T. W. Li, and P. H. Kes, Phys. Rev. B **51**, 15492 (1995).
[25] M. Konczykowski, C. J. van der Beek, A. E. Koshelev, V. Mosser, M. Dodgson, and P. H. Kes, Phys. Rev. Lett. **97**, 237005 (2006).
[26] M. J. W. Dodgson, A. E. Koshelev, V. B. Geshkenbein, and G. Blatter, Phys. Rev. Lett. **84**, 2698 (2000).
[27] K. Kimura, R. Koshida, W. K. Kwok, G. W. Crabtree, S. Okayasu, M. Sataka, Y. Kazumata, and K. Kadowaki, J. Low Temp. Phys. **117**, 1471 (1999).
[28] V. M. Vinokur, V. B. Geshkenbein, A. I. Larkin, and M. V. Feigel'man, Zh. Eksp. Teor. Fiz. **100**, 1104 (1991).
[29] D. Fuchs, E. Zeldov, M. Rappaport, T. Tamegai, S. Ooi, and H. Shtrikman, Nature (London) **391**, 373 (1998).
[30] M. Konczykowski, C. J. van der Beek, A. E. Koshelev, V. Mosser, M. Li, and P. H. Kes, J. Phys.: Conf. Ser. **150**, 052119 (2009).
[31] B. Khaykovich, E. Zeldov, D. Majer, T. W. Li, P. H. Kes, and M. Konczykowski, Phys. Rev. Lett. **76**, 2555 (1996).
[32] I. Sochnikov, A. Shaulov, and Y. Yeshurun, J. Appl. Phys. **103**, 07C705 (2008).
[33] C. J. van der Beek, M. V. Indenbom, V. Berseth, T. W. Li, and W. Benoit, J. Low Temp. Phys. **105**, 1047 (1996).
[34] M. Konczykowski, S. Colson, C. J. van der Beek, M. V. Indenbom, P. H. Kes, and E. Zeldov, Phys. C (Amsterdam, Neth.) **332**, 219 (2000).